

---

## Reuse of livestock waste for the reinforcement of rammed-earth materials: investigation on mechanical performances

Monica C. M. Parlato, Carlos Rivera-Gómez, Simona M.C. Porto

---

### Publisher's Disclaimer

E-publishing ahead of print is increasingly important for the rapid dissemination of science. The *Early Access* service lets users access peer-reviewed articles well before print/regular issue publication, significantly reducing the time it takes for critical findings to reach the research community.

These articles are searchable and citable by their DOI (Digital Object Identifier).

Our Journal is, therefore, e-publishing PDF files of an early version of manuscripts that undergone a regular peer review and have been accepted for publication, but have not been through the typesetting, pagination and proofreading processes, which may lead to differences between this version and the final one.

The final version of the manuscript will then appear on a regular issue of the journal.

*Please cite this article as doi: 10.4081/jae.2023.1434*

 ©The Author(s), 2023  
Licensee [PAGEPress](#), Italy

Submitted: 28/04/2022

Revised: 27/06/2023

Accepted: 06/07/2022

*Note: The publisher is not responsible for the content or functionality of any supporting information supplied by the authors. Any queries should be directed to the corresponding author for the article.*

*All claims expressed in this article are solely those of the authors and do not necessarily represent those of their affiliated organizations, or those of the publisher, the editors and the reviewers. Any product that may be evaluated in this article or claim that may be made by its manufacturer is not guaranteed or endorsed by the publisher.*

**Reuse of livestock waste for the reinforcement of rammed-earth materials: investigation on mechanical performances**

Monica C. M. Parlato,<sup>1</sup> Carlos Rivera-Gómez,<sup>2</sup> Simona M. C. Porto<sup>1</sup>

<sup>1</sup>Department of Agriculture, Food and Environment, University of Catania, Catania, Italy;

<sup>2</sup>Department of Architectural Constructions 1, Higher Technical School of Architecture, University of Seville, Seville, Spain

**Correspondence:** Monica C. M. Parlato, Department of Agriculture, Food and Environment, University of Catania, Building and Land Engineering Section (Di3A), University of Catania via S. Sofia 100, 95123 - Catania, Italy. E-mail: [monica.parlato@unict.it](mailto:monica.parlato@unict.it)

**Key words:** Building sustainability; raw earth materials; livestock waste; sheep wool fibers; mechanical behaviors.

## **Abstract**

Agricultural wastes as additive within raw earth materials could both improve mechanical and physical properties of new sustainable construction materials and enhance waste management in a circular economy perspective. This study intends to fill the lack of knowledge considering the mechanical effects of animal fibers on rammed earth materials. The effects of a livestock waste, i.e., sheep wool fiber (SWF), as reinforcing element in building components produced by using raw earth and lime-free mortars, have been evaluated. The samples were made by varying the content of wool (0.25 % or 0.50% weight) and the length of the fibers (from 10 mm to 40 mm). Linear shrinkage, flexural strength, compressive strength, and fracture energy were evaluated on samples incorporating SWF, with the aim of assessing the effects of this waste addition on the mechanical performances of a new bio-composite material. The best result of the flexural strength was 1.06 MPa, exhibited by samples made with the longest and highest percentage of fibers, 40 mm and 0.50%, respectively. The average compression strength was about 3.00 MPa. The average energy fracture of the composite was 806.38 [N/mm].

## **1 Introduction**

Today, the construction sector, is the leading cause of environmental degradation, global warming, and climate change, with 50% of carbon emissions, 20% to 50% of energy and natural resource consumption, and 50% of the total production of solid waste (Vasilca et al., 2021). For this reason, the attention of researchers and technicians in new alternative construction materials derived from renewable sources is growing constantly (Bonoli et al., 2021).

In this context, the interest in earthen construction materials is increasing both for the restoration of existing historical and cultural built heritage and new constructions. Several advantages come from the use of raw earth-based materials, all related to a significant decrease in environmental pollution and CO<sub>2</sub> emissions. Raw earth building components, if made without chemical additives (i.e., only by physical and mechanical stabilization), are totally recyclable (Achenza and Sanna, 2009; Parlato

et al., 2021). Generally, raw earth-based building components are extracted and worked directly or close to the building site, so their use significantly reduces logistic and transportation costs and the related gas emissions. Compared to common building materials (i.e., concrete, steel, glass) raw earth-based materials are suitable to balance and control indoor acoustic and thermal comfort (Fagone et al., 2019).

To improve earthen materials behaviour, additives or stabilizers are often used to design raw mixes, such as mineral binders (cement, alginate, bitumen) (Rivera-Gómez and Galán-Marín, 2017; Turco et al., 2021), animal and vegetal stabilizers (oil, casein, animal glue, latex) (Medvey and Dobszay, 2020), reinforcement fibers, synthetics, or natural (Eliche-Quesada et al., 2017; Ramesh, 2016). Several studies focused their attention on Agricultural Waste (AW) and on their high potential use in different construction applications, all with the aim of minimizing their production and promoting environmental sustainability (Barreca et al., 2019; Liuzzi et al., 2017; Reif et al., 2016). When considering their significant mechanical and physics performances, AW are suitable as alternative materials in the building sector and are considered the most sustainable, economical, and energy efficient resources (Jannat et al., 2020).

Many scientists have evaluated the use of AW as natural additives in the field of unfired earth materials (Araya-Letelier et al., 2018; Serrano et al., 2016; Vatani Oskouei et al., 2017). These studies focused mainly on agro-waste fibers (e.g., straw fibers, Hibiscus cannabinus fibers, ground olive stones, wheat straw fibers) (Salih et al., 2020). The main advantage of fiber reinforcement is to improve the mechanical properties, shrinkage rate, and ductility of the composite (Laborel-Préneron et al., 2016; Parisi et al., 2015; Vega et al., 2011).

The major part of paper are related to the addition of vegetable fibers to rammed earth, fewer researchers have evaluated the mechanical effects of reinforcements of animal fibers (e.g., pig hair, sheep wool) (Araya-Letelier et al., 2018; Statuto et al., 2018).

In the framework of sustainable use of natural resources, raw sheep wool is reconsidered as a renewable resource by converting a difficult waste into a value-added material. In Europe in 2011,

the estimated production of raw sheep wool based on sheep number was about 260,000 tons. In Italy, the estimated annual production of raw wool is around 14,000 tons, of which only a small part, around 5%, is suitable for the textile industry and has a commercial value (Rajabinejad et al., 2019).

A large amount of raw sheep wool that is not suitable for the market represents for sheep farmers a relevant issue due to the complexity and difficulty of the disposal management. Moreover, the increasing waste landfill fees is often the main reason of the illegal disposal of raw sheep wool (Saxena and Sewak, 2016). In accordance with European Environmental Regulations (EC Regulation 1069 (2009), EU Regulation 142 (2011)), raw sheep wool must be sent to specialized sites for incineration or landfill, and only if it is previously washed or disinfected, it can be buried or burned without a permit. The valorization of this livestock waste, the complex disposal, as components of building elements, is in turn sustainable both from the point of view of reducing CO<sub>2</sub> emissions in the production process and of reducing energy costs for managing the construction. Wool fibers, obtained by raw wool generally washed with natural soap, in form of soft mats or loose wool, could be used as thermal and acoustical insulation of buildings, as reinforcement fiber for composite materials, as sorbent materials for the treatment of water pollution, etc. (Dénes et al., 2019).

This study refers to the possible reuse of raw sheep wool, trying to partially fill the lack of knowledge about the effects of animal fiber reinforcement on rammed earth materials.

In this paper, the use of short wool fibers as reinforcing elements of non-structural building components is proposed in combination with eco-sustainable materials such as raw earth and lime-free mortars.

The research gap that this paper attempts to address and, therefore, the novelty of the study, lies in the combination of animal fibers with binders that do not use cement or lime to reduce the impact resulting from the production processes. In addition, results involve comprehensive examination through cross comparison of mechanical performance to obtain in-depth information with the goal to propose these new materials as an alternative to other more common earthen products reinforced with plant fibers. The attempt is to evaluate effects deriving by the addition of this waste to unfired

materials made with clay soil present in Sicily, which was formerly used to produce bricks, and mixed up with a pyroclastic sand. This pyroclastic sand is typical of the Etna volcano area located in Sicily (Italy) and is commonly used to increase the mechanical strength in mortar and concrete products. The design of the raw earth mix was prepared by performing only a physical stabilization, without the use of chemical additives, by obtaining a material that is totally recyclable at the end of its useful life (Parlato et al., 2021). The elements that we propose to develop could be used as closing elements. Then, with the aim of avoiding the use of chemical additives, the present work investigates the application of a promising natural fiber, i.e., sheep wool fiber, for rammed earth stabilization, including their influence on the mechanical properties of the material. The main purpose is to find the most performant design for both fiber length and percentage. Then, physical, and mechanical tests were carried out to obtain information related earthen material. Other interesting aspects that could be in the future investigate are concerning the durability of the material, its thermal properties, and interaction among fibers and the matrix soil by SEM analyses. Finally, the results have been compared with those of other studies that investigated other agricultural waste additives.

## **2 Materials and Methods**

Experimental tests on the physical and mechanical behavior of raw earth-based materials were reported under flexural and compression tests. Since the mechanical behaviors of the raw earth building components are sensitive to both soil composition and fiber content, the length and percentage of the SWF were changed to evaluate the best mix design. According to the results obtained, the reinforcement by fibers is essential to confer the due ductility to the bio-compound. First, test samples were performed by using the same soil mix design and varying only the fiber content (0,25% or 0,50%) and the length of the fibers (from shorter fibers of 10 mm to longer fibers of 40 mm).

### **2.1 Clayey Soil and Volcanic Sand**

Experimental tests were carried out on a soil mix previously investigated by authors (Parlato et al.,

2021); this soil, chosen among five different soil design for its best performances, was embedded with raw sheep wool. The base material is composed of kaolinite soil called *terra di Floridia* (FS) (extracted close to Syracuse in Sicily and traditionally used to produce bricks) modified through a physical stabilization process (Achenza and Sanna, 2009) to improve its mechanical behavior.

The particle size distribution of FS has been changed through the addition of clay, in the proportion of 58% FS soil and 42% clay, in weight. In literature good results have been achieved with a similar soil composition (Galán-Marín et al., 2013). Clay improves plasticity, mechanical characteristics, and cohesion, and can reduce water absorption enhancing erosion resistance to wind and waterproofing toward capillarity water.

The clay used for the stabilization process comes from a pit located near Misterbianco, in the province of Catania (Italy). The basic components used for the casting of the samples were chosen for their chemical and mechanical properties and favoring local materials with a consequent reduction in logistic and transport costs. Subsequently, to improve its mechanical resistance, and prevent shrinkage and cracking problems, the modified '*Terra di Floridia*' (FS<sup>M</sup>) has been mixed with a typical pyroclastic sand, sieved to 2 millimeters of the Etna volcano area (Sicily) and commonly used to produce mortars and concretes. On a dry weight basis the rate was 45% of sand and 55% of FS<sup>M</sup>, the final design, including water, was 45% FS<sup>M</sup>, 35% sand, 20% water. In a previous work conducted by authors, this mix obtained the best mechanical performances among five different mix (Parlato et al., 2021). This characteristic sand called '*azolo*' is formed on the surface of the lava by crushing glassy materials generated by rapid cooling of the magma. Table 1 shows the chemical composition of clay and volcanic sand added to FS.

*Table 1-chemical composition of clay and volcanic sand*

Sieve analyses were carried out in an earlier study (Parlato et al., 2021) according to ASTM D7928 – 17 requirements in order to determine the particle size distributions of FS and clay (**Error! Reference source not found.****Error! Reference source not found.**a and 1b). **Error! Reference source not found.** c shows the particle size distribution of the soil mix FS<sup>M</sup>, and Figure 2 d the

particle size of the final mix (including additive sand).

## 2.2 Livestock waste as reinforcement fibers: sheep wool

The livestock waste used in this investigation is typical raw wool from Sicilian sheep of the '*Valle del Belice*' race, widespread in this region, whose fleece, thick and medium length, is rejected by the textile industry. In the recent past, these fibers were suitable for mattress and/or pillow production, but currently they are only considered special waste with high disposal costs for breeders.

Sheep wool fibers used as reinforcement fibers, that is, '*Valle del Belice*' fleece, is a very coarse wool, with diameter ranged around 70.0  $\mu\text{m}$ . These fibers were physically and mechanically characterized by the authors in a recent study (Parlato et al., 2022). A selection of about 180 fibers were measured (length and mass), and after tensile tests were performed on selected fibers.

Due to the high hydrophilic content of wool, three different conditioning programs (wet, dry, and intermediate condition) were carried out and compared, with the aim of acquiring useful information about the maintenance of the mechanical properties in wet environments like those present in lime mixes. By considering three different test settings: wet condition, controlled environment, oven-dried condition SWF tensile performances were studied. Secant Stiffness Modulus ( $E_s$ ), Stress ( $\sigma_y$ ) and strain ( $\varepsilon_y$ ) at the yield, Elongation at break ( $E_b$ ), Stress at break ( $\sigma_b$ ) are the mechanical properties evaluated from each test. Average values  $\mu_i$  and standard deviations  $\sigma_i$  for these quantities, are reported in Table 2, separately for the three testing conditions and for the whole population. Although the tests produced very similar results, better results have been obtained for the fibers tested under the second experimental condition, that is, in a controlled environment (SWF immersed in distilled water for ten minutes and left to dry for 24 h in ambient with temperature and humidity monitored). The results obtained appear to support the use of SWF as a reinforcing material because this second conditioning procedure is close to the real condition of fibers inside a mixture of an earth-based composite. Average tensile strength obtained was 137.31 MPa, elongation at break 42.00 %. These values are comparable with wool tensile strength found in literature ranged between 120 and 174



MPa, and higher respect the elongation at break ranged between 25 and 35 %, (Cheung et al., 2009). Compared to other natural fibers, for example, jute and sisal with an average tensile strength of 249 MPa and 484 MPa (Alves Fidelis et al., 2013), respectively, wool exhibits a lower strength, while the elongation at break is higher than the most commonly natural fibers used as reinforcement material (Ku et al., 2011).

The percentage of fibers used in the mix ranged between 0,25 % and 0,50 %, in weight. This low percentage in weight corresponds to a larger volume of fibers due to the low density of this kind of wool (average density of 0.94 gr/cm<sup>3</sup>).

The length of the fibers varies between 10 - 40 mm, to evaluate the possible effects caused by the different lengths on the mechanical behaviours of the samples.

In Figure 2 (a and b) shows a Scanning Electron Microscopy (SEM) analysis of wool fibre surface and transversal section. SEM analysis was carried out at “*Torre Biologica*” of University of Catania .

### 2.2.1 Adobe mix sample preparation

The preparation of the samples began with the addition of fibers to the homogeneous soil mix, that is, FS<sup>M</sup> and sand. All specimen's preparation and compaction process have been executed manually (**Error! Reference source not found.**). Since manual compaction was adopted, the compaction energy was not monitored, but the manufacturing water content of the soil was controlled while mixing. For each formwork, the same amount of mix was casted, to obtain the design density of 1800 kgm<sup>-3</sup>.

SWFs were slowly and carefully added to the clay soil to reduce the formation of fiber bundles. In the end, once the fibers were fully incorporated into the mixes, water was added in four steps, manually stirring between each step. The samples were cast in consecutive layers and compacted by hand applying sufficient pressure. Three days after casting, the samples were demolded and put in dry and aired storage area (AT= 26° C, ARH=60 %) for 28 days to cure before testing. Moreover, after this time the specimens 'weight difference of two consecutive readings (24hours) was constant

( $\pm 0.01\text{g}$ ). A similar curing procedure is in accordance with the New Zealand Code (NZA 4298, 1998) and was used in previous research, also with non-cement stabilized earth samples (Parlato et al., 2021). After curing time, the weights and dimensions of each sample were measured, and then the densities were evaluated.

As stated above, to perform a sensitivity analysis on the impact of different fiber lengths and dosages on the performance of adobe mixes, SWF was cut in length (from 10 mm to 40 mm) and mixed in dry soil at a 0.25% or 0.50% per dry weight of soil. Nine different combinations of mixes, with six repetitions for each mix, were tested to assess the influence of SWF addition on the design of the adobe mix. In table 3 are reported the different mix tested within this study identified by the related ID. Mix identified with ID 0 was the control sample, mix identified with ID XX-YY incorporated fiber XX mm length at a rate of 0, YY%.

## 2.3 Mechanical and physical performances

### 2.3.1 Flexural and Compressive test

According to European standards (EN 1015-11:2019) for the mechanical testing of moulded mortar specimens, prismatic samples (160 mm  $\times$  40 mm  $\times$  40 mm) were prepared. To prevent adherence, the standard steel molds used were previously moistened.

Nine different combinations of mixes, named and listed in **Error! Reference source not found.**, with six repetitions for each mix, were tested to assess the influence of SWF addition on the design of the adobe mix. The samples were manufactured by changing both the length and percentage of fiber.

First, mechanical assessment began with the flexural tests. Using a Universal Testing Machine (UTM) connected with a Load Cell Hottinger Baldwin performed the test; Catman Software for Tests with Huge Channel Counts implemented data acquisition. Applying a single point load at the mid-span performed flexural tests, the speed of load was 10 N/s. Load values were recorded from the start until the sample failure. The Prismatic specimens were placed on two lower roller supports (100 mm

wheelbase). By using Equation 1 the flexural strength of specimen ( $\sigma_f$ ) was evaluated.

$$\sigma_f = \frac{3FL}{2bd^2} [MPa] \quad (1)$$

where  $F [N]$  is the maximum applied load,  $L [mm]$  is the span between supports (100 mm),  $b [mm]$  is the width of the specimen at the mid-section and  $d [mm]$  is the average depth of the specimen at the fracture section.

After failure, the compressive test on the two remaining prismatic parts obtained after the flexural fracture was performed. In order to avoid the concentrations of applied forces through particular points of the specimens, due the presence of irregularities on the surface of the samples (Ciancio et al., 2013), the two remaining parts tested under compression have been positioned on the side part with a level surface. This level and even end surface was obtained thank the steel mold used for the casting process, previously moistened. Samples kept the same flexural ID by adding numbers 1 or 2. To determine compressive strength value ( $\sigma_c$ ) Equation 2 was apply:

$$\sigma_c = \frac{F}{S} [MPa] \quad (2)$$

where  $F [N]$  is the maximum applied load and  $S [mm^2]$  is the surface of the loaded section. In both cases, i.e., flexural, and compressive test, the breaking loads were determined in correspondence with the maximum load reached during the tests.

### **2.3.2 Linear Shrinkage**

Linear shrinkage test was carried out in accordance to testing method ASTM C326-09 suitable for earthen materials. To evaluate linear shrinkage the dimensions of the prism mould length ( $L_i$ , mm) were measured. After 28 days, corresponding to the drying period, the dimensions of the prism sample

length ( $L_d$ , mm) were recorded using a digital calliper.

The linear drying shrinkage ( $S_d$ ) is calculated by using Equation (3):

$$S_d = \frac{L_i - L_d}{L_i} \times 100 \quad (3)$$

where  $L_i$  [mm] is the drying length of the specimen, measured by using a digital calliper, and  $L_d$  [mm] is the internal length of the mould.

### 2.3.3 Fracture Energy

In this study, to determine the fracture energy of raw earth samples reinforced with sheep wool fibers, a uniaxial flexural test was carried out with displacement control and load speed of 0.5 N/s. The fracture energy was calculated as the area under the load-displacement curve and was considered as the energy absorbed by the material until the deflection at the final fracture of the beam and considering the Petersson correction (Tvbm and Materials, 1982) to this area under the load-displacement curve two areas were added evaluated considering the force energetically equivalent to the weight of the samples. In **Error! Reference source not found.** is shown a typical flexural test on a sample.

$$G = \frac{W_0 + W_1 + W_2}{A_{lig}} \quad [\text{Nmm}^{-1}] \quad (4)$$

**Error! Reference source not found.** shows a diagram to evaluate the energy fracture. To calculate the fracture energy has been applied equation 4. Where  $G$  is the energy fracture,  $W_0$  the area under the experimental load displacement curve,  $W_1$  and  $W_2$  are the area evaluated considering the weight of the sample between supports. In detail,  $W_1$  is equal to  $F_0 \delta_0$ , i.e.,  $F_0$  is the sample mass (between supports) and  $\delta_0$  the last displacement, and  $W_2$  is supposed equal to  $W_1/2$ .  $W_3$  is considered negligible

and equal to zero.  $A_{lig}$  is the surface area of the notch, in this study  $A_{lig}$  was assumed equal to the lower surface of sample because they were realized without notch. Flexural tests have been carried out on mixes ID 0, ID 10 – 50, ID 30 – 50 (SWF 0.50% -30 mm), and ID 40 – 50 (SWF 0.50% - 40 mm), made by keeping constant the percentage of wool and varying its length.

### 3 Experimental Results and discussion

#### 3.1 Effect of sheep wool addition on Flexural Strengths

**Error! Reference source not found.** shows the average flexural strengths of each one of the nine-mix tested after casting, also including the minimum value and the maximum value measured. As usually happens with natural materials, the results are quite dispersed with average values of flexural strength ranging from 1.06 MPa and 0.50 MPa.

In general, the average flexural strength of adobe mixes decreases when sheep wool was introduced into the mix. These reductions respect ID 0 was of 23% for ID 10-25, of 12% for both mix ID 10 – 50 and ID 20-25, of 24 % for ID 20-50, of 43% for ID 30-25, of 21% for ID 30-50. Samples realized with ID 40-25 obtained a result comparable with strength of the control samples, respectively 0.88 MPa and 0.89 MPa, and mix ID 40 – 50 registered the highest average flexural strength of 1.06 MPa, with an increment of the 16% respect mix ID 0. The standard deviation values varied from 0.16 MPa (ID 10-50) to 0.23 MPa (ID 20-50).

These results have been compared to those previously reported for unfired reinforced adobe, despite in literature there are few studies regarding the flexural strength of raw earth materials. (Araya-Letelier et al., 2018) in their study carried out investigations on mechanical properties of unfired adobe reinforced with pig hair. They found a flexural strength ranged from 0.34 MPa to 0.49 MPa.

Galan-Marin et al. (Galán-Marín et al., 2010b) in their study evaluated the flexural strength of adobe realized by a clay soil incorporating 0.25% of raw wool, 10 mm long fibers. The average flexural strength obtained was of 1.10 MPa.

In the present work, the reduction in average flexural strength as sheep wool is introduced in the mix is explained by the generation of fiber clusters inside the composite matrix. This same trend was registered in other researches (Araya-Letelier et al., 2018; Baeza et al., 2013) that ascribe this negative effect of cluster formation inside the mix. Clusters avoid a complete adhesion between fibers and the matrix by affecting the average strength of the composite material. On the contrary mix realized with longer fiber exhibit a flexural strength comparable (ID 40-25) or higher (ID 40-50) than flexural strength of control sample. The reason is on the higher contact surface among the longer fibers and the matrix, as already explained in literature (Aymerich et al., 2012; Oliver-Ortega et al., 2018). Moreover, as the fiber is added by weight, by considering the same percentage of fiber, it is necessary to underline that the number of fibers inside the specimens increase for shorter fiber; it is assumed that the 10 mm fibers are 4 times the number of 40 mm fibers. The higher the number inside the mix the higher the possibility of cluster formation.

In any case, all adobe mixes exhibited an average flexural strength higher than the minimum values required by the worldwide used raw earth regulations, e.g., the New Mexico Earthen Building Materials Code, that foreseen an average minimum flexural strength of 0.35 MPa.

### **3.2 Effect of sheep wool addition on compressive strenghts**

The compressive strength of raw earth materials is considered a basic mechanical parameter to be considered depending on various parameters, such as compaction energy, manufacturing water content, dry density, stabilization process (Arrigoni et al., 2018; Bruno Agostino, Walter Galipoli, 2015). Figure 7 shows average values of results for the compressive test, including minimum and maximum values and standard deviation. Each value represents the average of a total of 12 specimens. The compressive strength values are less dispersed respect to flexural strength values, with average ranging from 2.58 MPa to 3.67 MPa, not considering specimens made with mix ID 30 -25 that registered a value of 1.42 MPa lower of the 53% respect ID 0. The lowest values of both flexural and compressive strength registered by mix ID 30 – 25 could be explained in some irregularities occurred

during the manufacturing process of the specimens, so authors have decided to discard this batch in final conclusions.

Despite all the specimen preparation process is manual, in the future could be important reach a minimum compression of soil, by using for instance a by hand press, to better compact the material and control its final behaviors and to avoid irregularities of the samples.

In this case introduction of fiber inside the mix doesn't cause a decrease in the average compressive strength, except for mix ID 30 -50 and ID 40-25, that registered a reduction respect the control mix of 15% and 3%. The best average compressive strength was obtained by mix ID 20-50, with an increment of almost the 15% if considering the control mix. The standard deviations varied from 0.13 MPa (ID 30-25) to 0.62 MPa (ID 10-50). Despite the values obtained for the mechanical properties of the unfired adobe considered in this study compare well with those reported in other scientific papers on similar fibers, Parlato et al. (Parlato et al., 2021) with the same mix of ID 0, so without fiber addition, found higher strengths values, i.e., 6.74 MPa for compressive strength and 1.65 MPa for flexural strength. The reason of this difference is due to the different condition of temperature and humidity. In the previous study the samples were produced during the winter season, with a temperature ranged between 13.1 °C -15.5 °C and air humidity between 76.7% - 80%, in this study specimens were molded during the summer season, with peak of temperature above 40° and a high thermal excursion during the day. So, the drying process was accelerated by this wethear condition compromising the final results. Galan-Marín investigated the effect of adding sheep wool and Lignum Sulfonate to raw-earth-based specimens and reported an increase of compressive strength of the 37% respect control sample, 2.23 MPa and 3.05 MPa, respectively (Galán-Marín et al., 2010a).

Statuto et al. (2018) evaluated the compressive strength of clay adobe brick reinforced by sheep wool fibers. They found that clay bricks mixed with 3% by weight of sheep wool exhibited an average compressive strength of 4.32 [MPa] (Statuto et al., 2018).

In any case, all compressive values found exceed the minimum compressive resistances foreseen by New Zealand Code and New Mexico Building Code, respectively 1.3 MPa and 2.1 MPa (New

Mexico, 2009; NZA 4298, 1998).

The high values obtained in the trials carried out within this study are mainly due to the soil mix that incorporates “azolo”, i.e., a siliceous inert, commonly used in the concrete industry, gives high resistance to compression.

The increment of the resistance is due to the chemical reaction of the pozzolanic material *Azolo*, before inert, induced by water addition into the mix. This chemical reaction produces Calcium Silicate Hydrate (CSH), a crystalline compound responsible for the material’s strength, and Calcium Hydroxide (CH), that acts as a filler and lines pores within the matrix in a manner like that of binding aggregates in concrete (Hossain et al., 2007).

In Table 4 mechanical results concerning the adobe mix tested in this study, included the dry density, are summarized.

The correlation between dry density and average compressive strength has been also investigated by excluding the outlier values referred to mix ID 30-25. An almost horizontal linear has shown in Figure 8.

The higher the density, the higher the compressive strength obtained by performing the test.

The direct correlation between density and compressive strength is widely accepted in literature (Kouakou and Morel, 2009; Pelé-Peltier et al., 2022).

When fibers are introduced into the mix, a quantity of soil is replaced by them. As expected, the bulk density of wool fibers is lower than the soil, addition of fibers led to a decrease in the earth content and thus in the composite dry density. Moreover, when fibers are added the dry density was lower and the material more porous. Several studies linking mechanical properties with porosity; compressive strength decreasing with increasing porosity (Al Rim et al., 1999; Ghavami et al., 1999; Sutcu et al., 2016)

Furthermore, compressive strength decreases due the weak adhesion among fibers and clay matrix.

Water absorption by fiber, occurs during the first 24 hours after molding, pushes away the soil. After drying, the volume of fibers decreases, and voids are created around them and the soil matrix. Fibers



could slip easily, reducing the homogeneity of the composite material (Khedari et al., 2005; Quagliarini and Lenci, 2010; Rivera-Gómez et al., 2014).

### **3.2.1 Statistical analysis of test results**

The mechanical resistances obtained through the performed trial were validated by a ONE-way analysis of variance (ANOVA) to determine if there is a statistically significant difference among the corresponding data means. A check of normality (by computing Shapiro-Wilk test) and homogeneity of variance (by computing Levene's test) preceded ANOVA. Statistical analysis has been performed by using RStudio (<https://www.rstudio.com/>) a free access software. The ANOVA test was performed both for flexural strength and compressive strength results.

In Table 5 and Table 6 are summarized results concerning the validation of flexural and compressive test, respectively.

In both cases p-value is above the significance level  $\alpha=0.05$ , i.e., 0.95 and 0.71, so not statistically significant. One-way ANOVA test revealed that the null hypothesis could be retained; there was not a statistically significant difference among the mean of the data set groups.

### **3.3 Effects of fibers addition on Linear Shrinkage**

Shrinkage is a physical phenomenon that refers to the drying process of the soil mixture caused by evaporation of moisture content; it determines the cracking of the material, which can increase the penetration of water, loss of strength, and material decay (Sangma and Tripura, 2020). Araya et al. (Araya-Letelier et al., 2018) determined shrinkage rate by using a different test procedure; test were carried out on two flat specimens and by a grid to control cracks distribution. They observed crack width reduction for both fiber dosage and fiber length increment.

Prismatic specimens tested within this study did not exhibit crack on the surface, only reductions on linear measures, and volume, were detected.

The Linear Shrinkage Test is a suitable tool for obtaining information about the shrinkage behavior

of raw earth materials, especially structural components to correctly anticipate the joint design of space construction (Ciancio et al., 2013). The requirements for the maximum shrinkage of rammed earth are identified, although the threshold values are discordant, for example the New Zealand Standard (NZA 4298, 1998) is 0.05 % and the German Lehmbau Regeln (Volhard, 2009) 2% . The linear shrinkage rate for the specimens concerning the different adobe mixes was evaluated by applying Equation 3. Samples made with soil mix ID 0 exhibited the highest shrinkage rate, corresponding to 6.25%.

*Figure 9 – Shrinkage rate for prismatic samples.*

The general trend is that the addition of fibers to the mix causes a decrease in the shrinkage rate, as already demonstrated in other research with comparative analysis among reinforced and unreinforced samples (Vega et al., 2011)

#### **3.4 Influence of reinforcement on the structural response of the material**

The quantity of energy necessary to generate and propagate a crack through a material is called the fracture energy. Fracture energy is the measure of how resistant a material is to crack formation, considering both instantaneous and long-lasting stresses.

However, fracture energy evaluation is not regulated by universal norms or laws, but there are only recommendations introduced by materials testing organizations (e.g., RILEM, ASTM); the most common experimental procedures use prismatic samples with or without notch (Volhard, 2009).

To investigate the structural response of the material in terms of first-crack resistance, post-cracking performance and energy absorption capability, flexural tests have been carried out on five different mixes, i.e., ID 0, ID 10 – 50, ID 30 – 50, ID 40 – 25, and ID 40 – 50, the mix with the higher percentage of wool. The fracture energy of the material was determined by using Eq. 4. In Table 7 the average results obtained for the different mix investigated in this study are reported. The peak load ( $F_{peak}$ ) ranges between 296.97 [N] and 529.00 [N]. The higher energy fracture was 959.89 [Nmm<sup>-1</sup>] exhibited by mix ID 30 – 50, the lower was 706.47 [Nmm<sup>-1</sup>] of mix ID 30 – 50. By

considering mix ID 0, it was observed that the last displacement  $\delta$  is equal to the peak displacement ( $\delta_{peak}$ ). Furthermore, it was not possible to determine its fracture energy because the unreinforced samples showed a rapid load drop with a complete loss of residual strength after the peak load.

The maximum value of Energy Fracture and of peak load was reached by mix ID 40-50,  $F_{peak}$  529.00 [N] and  $G_f$  959.89 [N/mm], the average value of Energy Fracture was 806.38 [N/mm].

**Error! Reference source not found.** shows a demonstrative set of Load–deflection curves ( $F$ - $\delta$ ) related mix ID 40-50.

The plot of this figure shows that reinforced samples have an almost linear initial response, characterized between origin and peak load.

All reinforced specimens present the same mechanical response to load; a linear initial phase until the peak load and a second phase characterized by a decreasing in load and high values of displacements; a falling load segment for large deflection value characterizes this second phase.

However, experimental results demonstrated that the addition of sheep wool fiber improves the ductility of the specimens; after failure, reinforced specimens exhibit the two parts linked together, while adobes realized without reinforcing fibers registered a sudden drop in load, because of the formation of unstable macroscopic crack after the maximum load. In fact, addition of fibers in the mix determines a redistribution of the internal forces. During the trial it was observed that the failure mode under flexural test was at the central axis; this means that samples were homogeneous with little discontinuities in the mass of the material. The failure mode occurs when the imposed load exceeds the flexural capacity of the material, i.e., flexural failure. The observed cracks, were vertical and were located in the middle of sample, these cracks were produced on the tension side of the prismatic specimens which further extend to the compression side. The flexural tension failure happened gradually, i.e., ductile failure. On the contrary, sample performed with mix ID 0 exhibited a fragile failure mode; after the peak load was observed a total loss of load carrying capability. The two parts of the specimen appear completely separately after failure (Figure 11).

A limited number of studies have been carried out to explore the influence of fibrous reinforcement

on ductility, fracture resistance, and post-fracture behaviour of earthen material (Clementi et al., 2008). Aymerich and co-workers (2012) investigated the improvements in strength and post-fracture performances by the introduction of wool fiber reinforcement in earthen material (Aymerich et al., 2012)a. They performed flexural tests on notched samples (prepared with two fiber weight fractions (2% and 3%) and different fiber lengths (1, 2, and 3 cm), to compare the mechanical response in terms of first-crack resistance, post-crack performance, and energy absorption capability. The results demonstrated that the fibrous reinforcement improved residual strength, ductility and energy absorption (Aymerich et al., 2012). Corbin et al. (2014) investigated the fracture energy of rammed earth by using the wedge splitting test, a test for calculating the fracture energy of concrete. As per obtained results, they found that adding cement increases the fracture energy of the material, but the addition of wool up a critical amount decreases it. The energy fracture evaluated was 0.71 N/m and 0.68 N/m for control samples made without cement and with wool addition of 1% and 2%, respectively. They used wool fibers from a carpet manufacturer cut into lengths of 30-50mm with an average tensile strength of 69.2 N/mm<sup>2</sup> (Corbin and Augarde, 2014). Recently, Mužíková et al. (2021) evaluated the fracture energy and strain-stress curve of three different sets of illite rammed earth. The highest value of the fracture energy found was of 4.858±0.002 J/m<sup>2</sup> (Mužíková et al., 2021).

One of the significant effects of the inclusion of natural fibres in the soil matrix is related to the failure mode of the specimen; in the case of the composite material, after the ultimate load was reached, the specimens still deformed and fine cracks could be seen on the surface of the specimens, on the contrary control specimen made without fiber addition broke quickly and almost without warning.

Under compression failure was characterized by the gradual formation of diagonal cracks on the lateral sides of the samples without an immediate failure after the peak load. The natural fibers held together significant parts of the soil matrix by delaying failure. Additionally, there was no rupture of the sheep fibers, although a loss of bond between the fibers and the soil matrix was recorded in the proximity of the cracks (Figure 12).

Under flexural test the stress–strain curve obtained is linear for all the test series up to maximum load.

For the natural soil the final failure occurs immediately after the ultimate load and for this reason it was not possible to evaluate the energy fracture of the material, that is estimated as the area under the stress-strain curve.

Mix ID 10-25 and ID 20-25 obtained the best average compression strength, 3.14 [MPa] and 3.13 [MPa], respectively; the best flexural strengths were obtained by the no fibrous mix with 0.89 [MPa] (mix ID 0), and by mix ID 40-25 with 0.88 [MPa]. In general, the average flexural strength of adobe mixes decreases when sheep wool was introduced into the mix, a different trend was obtained when the length and concentration of fibers increased (ID 40-50), the explanation found in literature is on the higher contact surface between fibers and clay matrix (Aymerich et al., 2012; Oliver-Ortega et al., 2018).

Another important aspect to be considered deriving by fiber addition is the prevention of visible shrinkage cracks due to the drying process. The Linear Shrinkage Rate decreases by fiber addition from ID 0 with a rate of 6.25 % to the minimum rate of 3.89%, registered by ID 10-50.

The addition of fibers to the mix determines the decrease in dry density from 1960.0 [kg/m<sup>3</sup>] to around 1845.00 [kg/m<sup>3</sup>] for mix ID 30-50 and ID 40-25 and 1883.0 for mix ID 40-50.

#### **4 Conclusions**

The agricultural sector produces a huge amount of waste, by-products, and co-products, whose disposal constitutes a serious financial and ecological concern.

This work assessed the effectiveness of incorporating a livestock waste, sheep wool fiber, as a reinforcement fiber in raw earth specimens. The purpose was to valorise local building materials and contemporary reduce a huge quantity of waste, and realize a totally recyclable material suitable for non-structural materials.

The final aim was to evaluate the most performant mix by contemporary consider fiber rate percentage and length. Basis on the mechanical trials, the best results have been exhibited by specimens realized with mix ID 40-50. However, all samples shown mechanical strength values

significantly higher than the minimum values required by the most relevant international regulation on raw earth material.

The high values obtained in this study are mainly due to the soil mix that incorporates a pozzolanic inert, '*azolo*', which gives increased resistance to compression and is traditionally used to improve mechanical strength in the production of concrete and mortar. *Azolo* soil reacting with clay minerals shape a variety of cement-like compounds binding soil particles together and at the same time reduce water absorption by clay particles.

Future research must fill the gap of this first investigation by exploring the acoustical and thermal behavior, the moisture absorption and desorption, and the durability of this raw earth materials reinforced with sheep wool fibers.

Moreover, a further detailed study should be able to evaluate, by means of Scanning Electron Microscope (SEM) and Energy Dispersive X-Ray (EDX) techniques, the fiber-matrix bonding for a better understanding its mechanical performance.

**Acknowledgements:** special thanks to Prof. Massimo Cuomo responsible of the Material Testing Lab of the University of Catania – (DICAR) where test have been carried out, and to Guglielmino Group (Misterbianco, CT) for samples' preparation.

**Funding:** The research study was funded by the University of Catania through the 'Piano incentivi per la ricerca di Ateneo 2020-2022-Linea 2' project on 'Engineering solutions for sustainable development of agricultural buildings and land' (ID: 5A722192152) (Acronym: LANDUS), Workpackage 2 "Sustainable buildings" coordinated by Simona M. C. Porto."

**Conflicts of Interest:** The authors declare no conflict of interest.

## References

Achenza, M., Sanna, U., 2009. Il Manuale tematico della terra cruda 126.

Al Rim, K., Ledhem, A., Douzane, O., Dheilily, R.M., Queneudec, M., 1999. Influence of the

proportion of wood on the thermal and mechanical performances of clay-cement-wood composites. *Cem. Concr. Compos.* 21, 269–276. [https://doi.org/10.1016/S0958-9465\(99\)00008-6](https://doi.org/10.1016/S0958-9465(99)00008-6)

Alves Fidelis, M.E., Pereira, T.V.C., Gomes, O.D.F.M., De Andrade Silva, F., Toledo Filho, R.D., 2013. The effect of fiber morphology on the tensile strength of natural fibers. *J. Mater. Res. Technol.* 2, 149–157. <https://doi.org/10.1016/j.jmrt.2013.02.003>

Araya-Letelier, G., Concha-Riedel, J., Antico, F.C., Valdés, C., Cáceres, G., 2018. Influence of natural fiber dosage and length on adobe mixes damage-mechanical behavior. *Constr. Build. Mater.* <https://doi.org/10.1016/j.conbuildmat.2018.04.151>

Arrigoni, A., Beckett, C.T.S., Ciancio, D., Pelosato, R., Dotelli, G., Grillet, A.C., 2018. Rammed Earth incorporating Recycled Concrete Aggregate: a sustainable, resistant and breathable construction solution. *Resour. Conserv. Recycl.* <https://doi.org/10.1016/j.resconrec.2018.05.025>

Aymerich, F., Fenu, L., Meloni, P., 2012. Effect of reinforcing wool fibres on fracture and energy absorption properties of an earthen material. *Constr. Build. Mater.* <https://doi.org/10.1016/j.conbuildmat.2011.08.008>

Baeza, F.J., Galao, O., Zornoza, E., Garcés, P., 2013. Effect of aspect ratio on strain sensing capacity of carbon fiber reinforced cement composites. *Mater. Des.* 51, 1085–1094. <https://doi.org/10.1016/j.matdes.2013.05.010>

Barreca, F., Martinez Gabarron, A., Flores Yepes, J.A., Pastor Pérez, J.J., 2019. Innovative use of giant reed and cork residues for panels of buildings in Mediterranean area. *Resour. Conserv. Recycl.* <https://doi.org/10.1016/j.resconrec.2018.10.005>

Bonoli, A., Zanni, S., Serrano-Bernardo, F., 2021. Sustainability in building and construction within the framework of circular cities and european new green deal. The contribution of concrete recycling. *Sustain.* 13, 1–16. <https://doi.org/10.3390/su13042139>

Bruno Agostino, Walter Galipoli, S.D., 2015. Briques de terre crue : procédure de compactage haute

pression et influence sur les propriétés mécaniques. 33èmes Rencontres l'AUGC, ISABTP/UPP, Anglet, 27 au 29 Mai 2015 1–9.

Cheung, H. yan, Ho, M. po, Lau, K. tak, Cardona, F., Hui, D., 2009. Natural fibre-reinforced composites for bioengineering and environmental engineering applications. *Compos. Part B Eng.* 40, 655–663. <https://doi.org/10.1016/j.compositesb.2009.04.014>

Ciancio, D., Jaquin, P., Walker, P., 2013. Advances on the assessment of soil suitability for rammed earth. *Constr. Build. Mater.* 42, 40–47. <https://doi.org/10.1016/j.conbuildmat.2012.12.049>

Clementi, F., Lenci, S., Sadowski, T., 2008. Fracture characteristics of unfired earth. *Int. J. Fract.* 149, 193–198. <https://doi.org/10.1007/s10704-008-9239-x>

Corbin, A., Augarde, C., 2014. Fracture Energy of Stabilised Rammed Earth. *Procedia Mater. Sci.* 3, 1675–1680. <https://doi.org/10.1016/j.mspro.2014.06.270>

Dénes, O., Florea, I., Manea, D.L., 2019. Utilization of Sheep Wool as a Building Material, in: *Procedia Manufacturing*. <https://doi.org/10.1016/j.promfg.2019.02.208>

Eliche-Quesada, D., Felipe-Sesé, M.A., López-Pérez, J.A., Infantes-Molina, A., 2017. Characterization and evaluation of rice husk ash and wood ash in sustainable clay matrix bricks. *Ceram. Int.* 43, 463–475. <https://doi.org/10.1016/j.ceramint.2016.09.181>

Fagone, M., Kloft, H., Loccarini, F., Ranocchiali, G., 2019. Jute fabric as a reinforcement for rammed earth structures. *Compos. Part B Eng.* <https://doi.org/10.1016/j.compositesb.2019.107064>

Galán-Marín, C., Rivera-Gómez, C., Bradley, F., 2013. Ultrasonic, molecular and mechanical testing diagnostics in natural fibre reinforced, polymer-stabilized earth blocks. *Int. J. Polym. Sci.* <https://doi.org/10.1155/2013/130582>

Galán-Marín, C., Rivera-Gómez, C., Petric-Gray, J., 2010a. Effect of animal fibres reinforcement on stabilized earth mechanical properties. *J. Biobased Mater. Bioenergy* 4, 121–128. <https://doi.org/10.1166/jbmb.2010.1076>

Galán-Marín, C., Rivera-Gómez, C., Petric, J., 2010b. Clay-based composite stabilized with natural polymer and fibre. *Constr. Build. Mater.* <https://doi.org/10.1016/j.conbuildmat.2010.01.008>



- Ghavami, K., Toledo Filho, R.D., Barbosa, N.P., 1999. Behaviour of composite soil reinforced with natural fibres. *Cem. Concr. Compos.* 21, 39–48. [https://doi.org/10.1016/S0958-9465\(98\)00033-X](https://doi.org/10.1016/S0958-9465(98)00033-X)
- Hossain, K.M.A., Lachemi, M., Easa, S., 2007. Stabilized soils for construction applications incorporating natural resources of Papua new Guinea 51, 711–731. <https://doi.org/10.1016/j.resconrec.2006.12.003>
- Jannat, N., Hussien, A., Abdullah, B., Cotgrave, A., 2020. Application of agro and non-agro waste materials for unfired earth blocks construction: A review. *Constr. Build. Mater.* 254, 119346. <https://doi.org/10.1016/j.conbuildmat.2020.119346>
- Khedari, J., Watsanasathaporn, P., Hirunlabh, J., 2005. Development of fibre-based soil-cement block with low thermal conductivity. *Cem. Concr. Compos.* 27, 111–116. <https://doi.org/10.1016/j.cemconcomp.2004.02.042>
- Kouakou, C.H., Morel, J.C., 2009. Strength and elasto-plastic properties of non-industrial building materials manufactured with clay as a natural binder. *Appl. Clay Sci.* 44, 27–34. <https://doi.org/10.1016/j.clay.2008.12.019>
- Ku, H., Wang, H., Pattarachaiyakoop, N., Trada, M., 2011. A review on the tensile properties of natural fiber reinforced polymer composites. *Compos. Part B Eng.* 42, 856–873. <https://doi.org/10.1016/j.compositesb.2011.01.010>
- Laborel-Préneron, A., Aubert, J.E., Magniont, C., Tribout, C., Bertron, A., 2016. Plant aggregates and fibers in earth construction materials: A review. *Constr. Build. Mater.* 111, 719–734. <https://doi.org/10.1016/j.conbuildmat.2016.02.119>
- Liuzzi, S., Sanarica, S., Stefanizzi, P., 2017. Use of agro-wastes in building materials in the Mediterranean area: A review, in: *Energy Procedia*. Elsevier Ltd, pp. 242–249. <https://doi.org/10.1016/j.egypro.2017.08.147>
- Medvey, B., Dobszay, G., 2020. Durability of Stabilized Earthen Constructions: A Review. *Geotech. Geol. Eng.* 38, 2403–2425. <https://doi.org/10.1007/s10706-020-01208-6>

- Mužíková, B., Otcovská, T.P., Padevět, P., 2021. Fracture energy of illitic rammed earth with high water-clay ratio. *Acta Polytech. CTU Proc.* 30, 53–57.  
<https://doi.org/10.14311/APP.2021.30.0053>
- New Mexico, 2009. New Mexico Earthen Building Materials Code. *Hous. Constr. Build. Codes Gen.*  
<https://doi.org/10.1017/CBO9781107415324.004>
- NZA 4298, 1998. New Zealand Standard: Materials and workmanship for earth buildings (NZS 4298: 1998).
- Oliver-Ortega, H., Llop, M.F., Espinach, F.X., Tarrés, Q., Ardanuy, M., Mutjé, P., 2018. Study of the flexural modulus of lignocellulosic fibers reinforced bio-based polyamide11 green composites. *Compos. Part B Eng.* 152, 126–132. <https://doi.org/10.1016/j.compositesb.2018.07.001>
- Parisi, F., Asprone, D., Fenu, L., Prota, A., 2015. Experimental characterization of Italian composite adobe bricks reinforced with straw fibers. *Compos. Struct.* 122, 300–307.  
<https://doi.org/10.1016/j.compstruct.2014.11.060>
- Parlato, M., Porto, S.M.C., Cascone, G., 2021. Raw earth-based building materials: An investigation on mechanical properties of Florida soil-based adobes. *J. Agric. Eng.* 52.  
<https://doi.org/10.4081/jae.2021.1154>
- Parlato, M.C.M., Cuomo, M., Porto, S.M.C., 2022. Natural fibers reinforcement for earthen building components : Mechanical performances of a low quality sheep wool ( “ Valle del Belice ” sheep ) 326.
- Pelé-Peltier, A., Fabbri, A., Morel, J.C., Hamard, E., Lhenry, M., 2022. A similitude relation to assessing the compressive strength of rammed earth from scale-down samples. *Case Stud. Constr. Mater.* 16. <https://doi.org/10.1016/j.cscm.2022.e00921>
- Quagliarini, E., Lenci, S., 2010. The influence of natural stabilizers and natural fibres on the mechanical properties of ancient Roman adobe bricks. *J. Cult. Herit.* 11, 309–314.  
<https://doi.org/10.1016/j.culher.2009.11.012>
- Rajabinejad, H., Bucîşcanu, I.I., Maier, S.S., 2019. Current approaches for raw wool waste

management and unconventional valorization: A review. *Environ. Eng. Manag. J.* 18, 1439–1456. <https://doi.org/10.30638/eemj.2019.136>

Ramesh, M., 2016. Kenaf (*Hibiscus cannabinus* L.) fibre based bio-materials: A review on processing and properties. *Prog. Mater. Sci.* <https://doi.org/10.1016/j.pmatsci.2015.11.001>

Reif, M., Zach, J., Hroudová, J., 2016. Studying the Properties of Particulate Insulating Materials on Natural Basis, in: *Procedia Engineering*. <https://doi.org/10.1016/j.proeng.2016.07.390>

Rivera-Gómez, C., Galán-Marín, C., 2017. Biodegradable fiber-reinforced polymer composites for construction applications, in: *Natural Fiber-Reinforced Biodegradable and Bioresorbable Polymer Composites*. <https://doi.org/10.1016/B978-0-08-100656-6.00004-2>

Rivera-Gómez, C., Galán-Marín, C., Bradley, F., 2014. Analysis of the influence of the fiber type in polymer matrix/fiber bond using natural organic polymer stabilizer. *Polymers (Basel)*. 6, 977–994. <https://doi.org/10.3390/polym6040977>

(<https://www.rstudio.com/>)

Salih, M.M., Osofero, A.I., Imbabi, M.S., 2020. Critical review of recent development in fiber reinforced adobe bricks for sustainable construction. *Front. Struct. Civ. Eng.* 14, 839–854. <https://doi.org/10.1007/s11709-020-0630-7>

Sangma, S., Tripura, D.D., 2020. Experimental study on shrinkage behaviour of earth walling materials with fibers and stabilizer for cob building. *Constr. Build. Mater.* 256. <https://doi.org/10.1016/j.conbuildmat.2020.119449>

Saxena, K.L., Sewak, R., 2016. Livestock waste and its impact on human health 6, 1084–1099.

Serrano, S., Barreneche, C., Cabeza, L.F., 2016. Use of by-products as additives in adobe bricks: Mechanical properties characterisation. *Constr. Build. Mater.* 108, 105–111. <https://doi.org/10.1016/j.conbuildmat.2016.01.044>

Statuto, D., Sica, C., Picuno, P., 2018. Experimental development of clay bricks reinforced with agricultural by-products. Sustainable Farming-SFARM View project Mediterranean technology led incubator co-operation-MEDI-CUBE View project.

- Sutcu, M., Ozturk, S., Yalamac, E., Gencel, O., 2016. Effect of olive mill waste addition on the properties of porous fired clay bricks using Taguchi method. *J. Environ. Manage.* 181, 185–192. <https://doi.org/10.1016/j.jenvman.2016.06.023>
- Turco, C., Paula Junior, A.C., Teixeira, E.R., Mateus, R., 2021. Optimisation of Compressed Earth Blocks (CEBs) using natural origin materials: A systematic literature review. *Constr. Build. Mater.* 309, 125140. <https://doi.org/10.1016/j.conbuildmat.2021.125140>
- Tvbm, R., Materials, B., 1982. the Fracture Energy of Concrete By Means of Three-Point Bend Tests on.
- Vasilca, I.-S., Nen, M., Chivu, O., Radu, V., Simion, C.-P., Marinescu, N., 2021. The Management of Environmental Resources in the Construction Sector: An Empirical Model. *Energies* 14, 2489. <https://doi.org/10.3390/en14092489>
- Vatani Oskouei, A., Afzali, M., Madadipour, M., 2017. Experimental investigation on mud bricks reinforced with natural additives under compressive and tensile tests. *Constr. Build. Mater.* 142, 137–147. <https://doi.org/10.1016/j.conbuildmat.2017.03.065>
- Vega, P., Juan, A., Ignacio Guerra, M., Morán, J.M., Aguado, P.J., Llamas, B., 2011. Mechanical characterisation of traditional adobes from the north of Spain. *Constr. Build. Mater.* <https://doi.org/10.1016/j.conbuildmat.2011.02.003>
- Volhard, F., 2009. *Lehmbau Regeln : Begriffe, Baustoffe, Bauteile / Verfasser: Franz Volhard, Ulrich Röhlen ; Dachverband Lehm e.V. (Hrsg.)*.No Title.

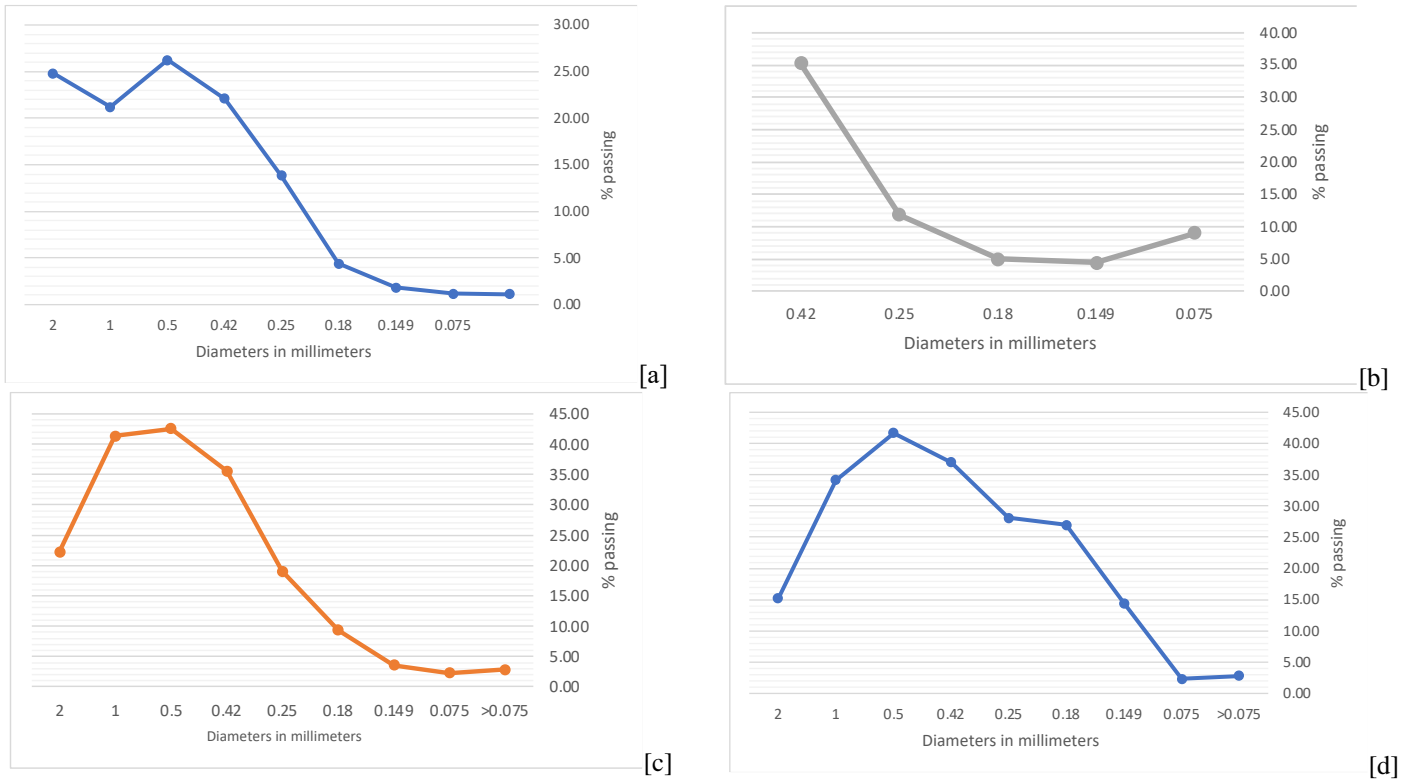


Figure 1- Particle size distribution of Florida soil (FS) [a], clay [b], size distribution of FS<sup>M</sup> [c], particle size of the final mix (including sand)

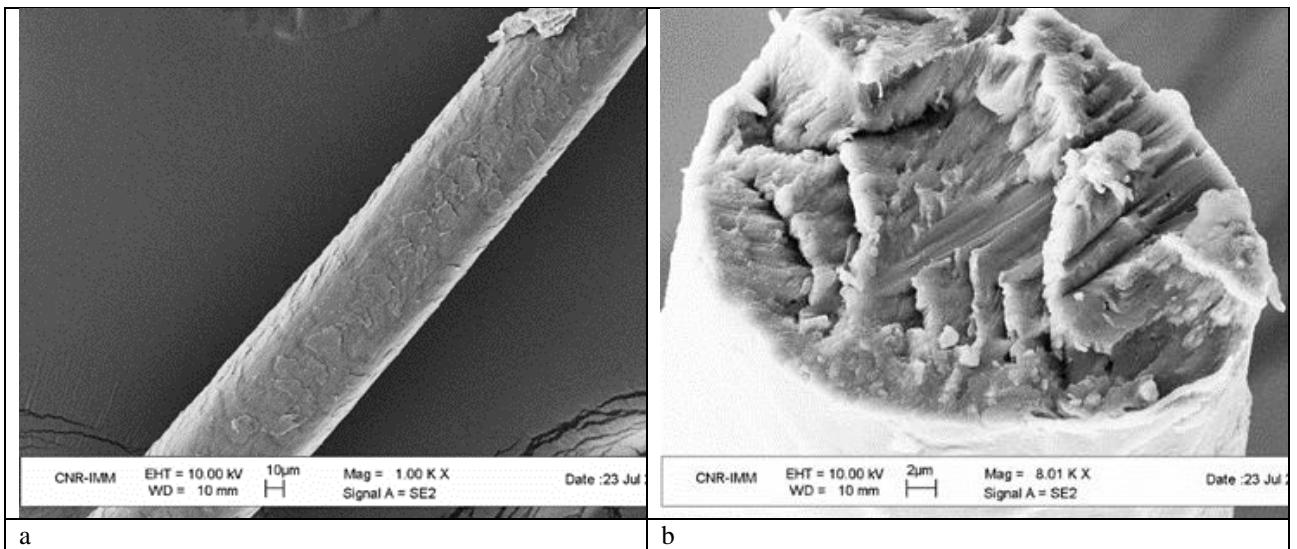


Figure 2 – SEM analysis of sheep wool fibre surface (a) and transversal section (b)



Figure 2- specimens tested in this study



Figure 3 - A sample ready for flexural test.

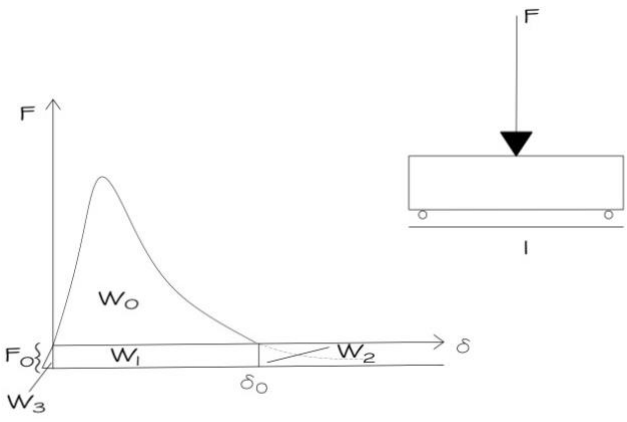


Figure 4 - Schematic force displacement diagram.

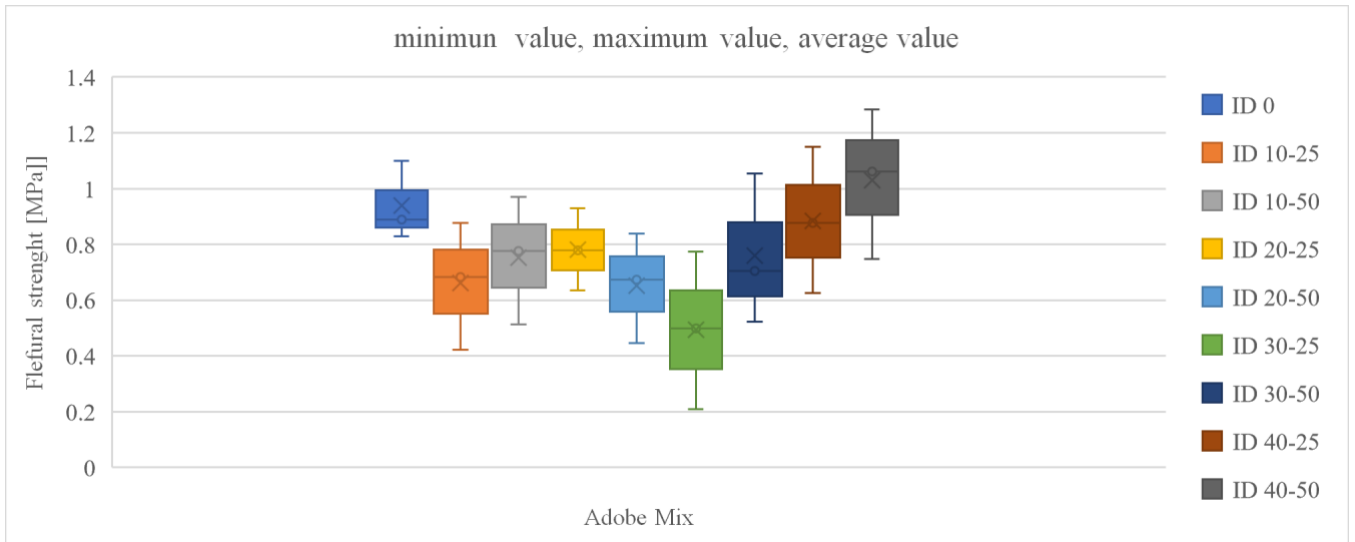


Figure 6 - Average values of flexural strength of the adobe mix, including minimum and maximum values for each mix

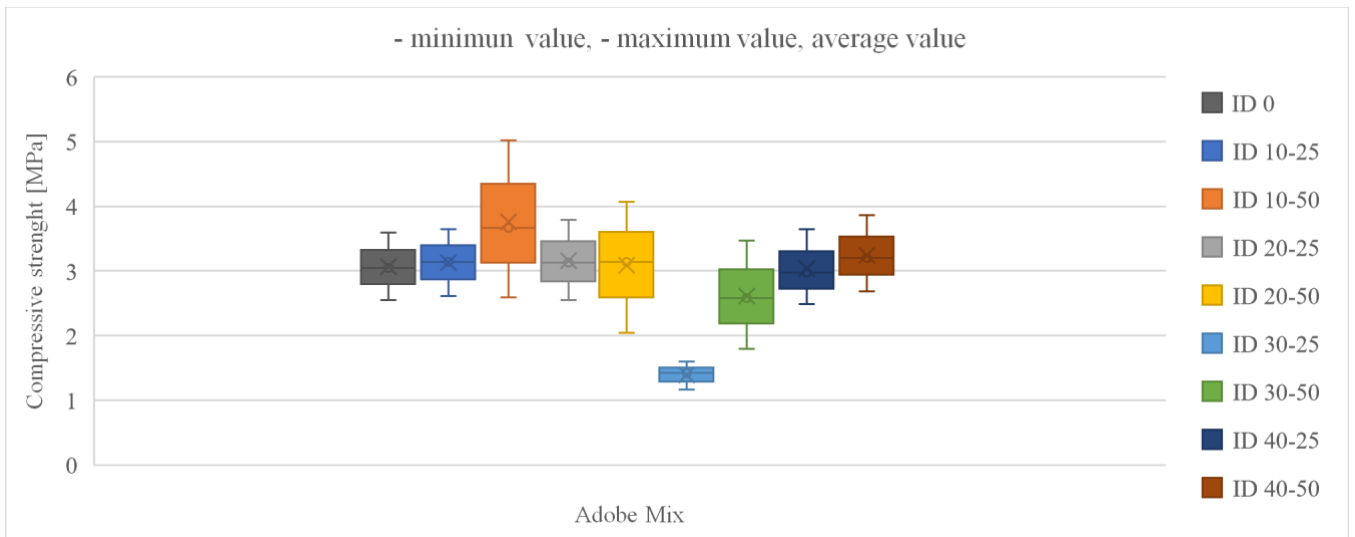


Figure 7 - Average values of compressive strength of the adobe mix, including minimum and maximum values for each mix

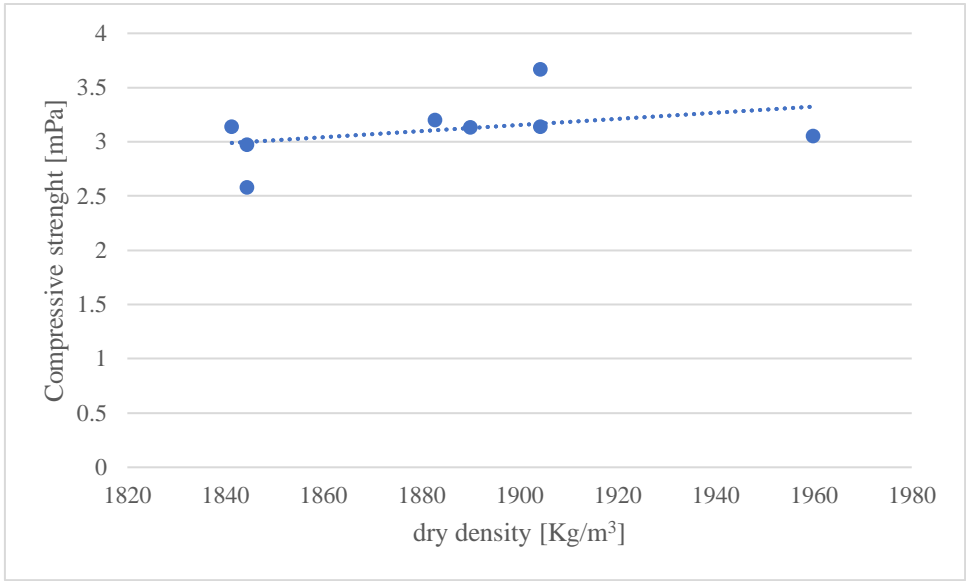


Figure 8 – Correlation among dry density and compressive strength

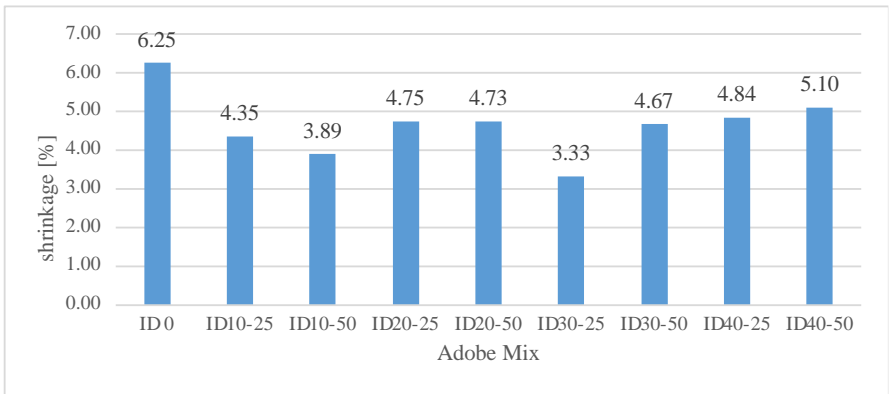


Figure 9 – Shrinkage rate for prismatic samples.

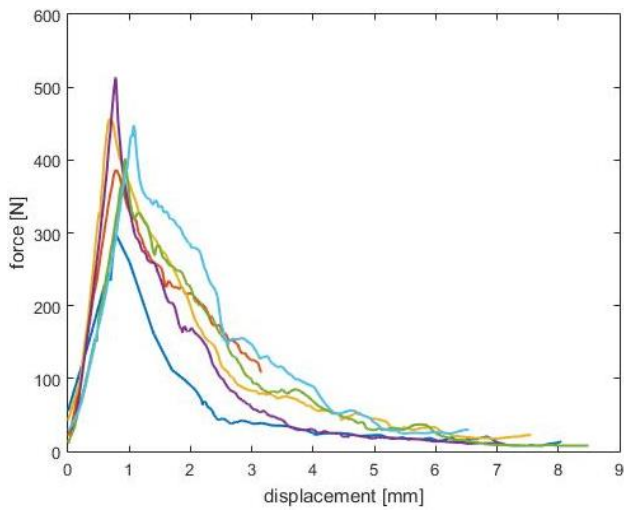


Figure 5 - Typical Set Load – Displacement curve for reinforced samples ( $F-\delta$ ),





*Figure 6 - failure mode of control sample (ID 0)*



*Figure 12 - composite specimens after compression test.*

**Table 2. Chemical composition of clay and volcanic sand.**

<b>Chemical Components</b>	<b>Clay [%]</b>	<b>Volcanic Sand [%]</b>
SiO <sub>2</sub>	53,15	45,9
Al <sub>2</sub> O <sub>3</sub>	14,42	20,43
TiO <sub>2</sub>	0,85	1,44
Fe <sub>2</sub> O <sub>3</sub>	6,09	9,99
MnO	0,10	0,15
MgO	2,13	4,71
CaO	7,21	10,22
Na <sub>2</sub> O	1,17	4,02
K <sub>2</sub> O	2,08	1,35
S	0,03	-
P <sub>2</sub> O <sub>5</sub>	0,16	0,48

**Table 2.**

	$\sigma_b$ [MPa]		$E_b$ [%]		$\sigma_y$ [MPa]		$\varepsilon_y$		$E_s$ [MPa]	
	$\mu$	$\sigma$	$\mu$	$\sigma$	$\mu$	$\sigma$	$\mu$	$\sigma$	$\mu$	$\sigma$
1. Saturated samples	134.57	34.10	42.00	0.11	75.37	21.92	0.04	0.02	2057.06	584.53
2. Normal conditioning	144.02	41.61	43.00	0.11	84.70	23.31	0.05	0.02	1903.59	621.32
3. Dry samples	133.65	47.22	43.00	0.19	85.97	33.59	0.07	0.03	1367.38	381.40
Entire population	137.31	41.37	42.00	0.14	81.44	27.15	0.05	0.02	1739.41	755.44

$\mu$  Average values;  $\sigma$  Standard deviation

**Table 3. Sample composition used for mechanical tests.**

<b>Mix</b>	<b>Wool lenght [mm]</b>	<b>Wool [%]</b>	<b>Soil* [%]</b>	<b>Water [%]</b>
ID - 0	-	-	80	20
ID 10 - 25	10	0.25	79.75	20
ID 10 - 50	10	0.50	79.50	20
ID 20 - 25	20	0.25	79.75	20
ID 20 - 50	20	0.50	79.50	20
ID 30 - 25	30	0.25	79.50	20
ID 30 - 50	30	0.50	79.50	20
ID 40 - 25	40	0.25	79.75	20
ID 40 - 50	40	0.50	79.50	20

\*Soil = FS<sup>M</sup> (55%) and volcanic sand (45%)

**Table 4. Average flexural and compressive strength with correlated standard deviation.**

Mix	Average flexural strength [MPa]			Average compression strength [MPa]			Average Dry density [kg/m <sup>3</sup> ]		
	$\mu$	$\sigma$	Coeff. of variance [%]	$\mu$	$\sigma$	Coeff. of variance [%]	$\mu$	$\sigma$	Coeff. of variance [%]
ID - 0	0.89	0.18	21.30	3.05	0.43	37.8	1960.0	923.4	49
ID 10 -25	0.68	0.16	23.09	3.14	0.29	9.30	1904.3	933.5	49
ID 10 - 50	0.78	0.16	20.91	3.67	0.63	17.00	1904.4	948.5	49
ID 20 - 25	0.78	0.17	22.33	3.13	0.35	11.10	1890.0	941.28	49
ID 20 - 50	0.67	0.23	34.97	3.14	0.62	19.00	1841.3	918.20	49
ID 30 - 25	0.50	0.20	40.00	1.42	0.13	9.00	1678.0	837.44	49
ID 30 - 50	0.70	0.19	27.35	2.58	0.47	18.00	1844.5	919.37	49
ID 40 - 25	0.88	0.19	21.44	2.97	0.35	11.10	1844.5	918.69	49
ID 40 - 50	1.06	0.20	19.70	3.20	0.40	12.00	1883.0	938.46	49

**Table 5. One-Way Analysis of Variance (ANOVA) of flexural strength test results, SSB: regression sum of square, SSW: total sum of squares (SSW=SSB+SSx), dfB: regression degrees of freedom (dfB= k-1), dfW: error degrees of freedom (dfW= n-k), k: total number of groups, n: total observations, MSB: regression mean square (MSB = SSB/dfB), MSW: error mean square (MSW = SSW/dfW), F: F test statistic (F = MSB / MSW), p: p-value that corresponds to FdfB, dfW.**

	Sum of Squares	df	Mean square	F	p-value
Between Groups (SSB)	0.30	7 (dfB)	0.04(MSB)	0.03	0.95
Sum Within groups (SSW)	66.53	40 (dfW)	1.66 (MSW)		

**Table 6. One-Way Analysis of Variance (ANOVA) of compressive strength test results SSB: regression sum of square, SSW: total sum of squares (SSW=SSB+SSx), dfB: regression degrees of freedom (dfB= k-1), dfW: error degrees of freedom (dfW= n-k), k: total number of groups, n: total observations, MSB: regression mean square (MSB = SSB/dfB), MSW: error mean square (MSW = SSW/dfW), F: F test statistic (F = MSB / MSW), p: p-value that corresponds to FdfB, dfW.**

	Sum of Squares	df	Mean square	F	p-value
Between Groups (SSB)	16.64	7 (dfB)	2.38 (MSB)	0.66	0.71
Sum Within groups (SSW)	319.12	88 (dfW)	3.63 (MSW)		

**Table 7. Average results for Energy Fracture for the different mix.**

Mix	$F_{peak}$ [N]	$\delta_{peak}$ [mm]	$\delta_0$ [mm]	$G_f$ [N/mm]
ID 0	398.00	4.28	4.28	-
ID 10 – 50	417.70	3.79	9.12	706.47
ID 30 – 50	296.97	4.22	8.58	752.79
ID 40 – 50	529.00	4.66	11.04	959.89
Average	410.41	4.24	8.25	806.38